In-plane dispersion of the quantum-well states of the epitaxial silver films on silicon

Iwao Matsuda and Toshiaki Ohta
Department of Chemistry, The University of Tokyo, Hongo, Tokyo 113-0033, Japan

Han Woong Yeom*
Atomic-scale Surface Science Research Center and Institute of Physics and Applied Physics, Yonsei University, Seoul 120-749, Korea
(Received 27 July 2001; published 8 February 2002)

In-plane dispersion of the quantum-well states (QWS's) associated with the electron confinement in metastable epitaxial Ag films grown on the Si(111)7×7 and Si(001)2×1 surfaces is investigated by angle-resolved photoemission using synchrotron radiation. In contrast to the free-electron-like behavior expected, these QWS's show intriguing dispersions such as (i) a significant enhancement of the in-plane effective mass with decreasing binding energy and (ii) a splitting of a QWS into two electronic states with different dispersions at off-normal emission. Such unexpected electronic properties of a QWS are obviously related to the substrate band structure. Further the QWS splitting is explained by the energy-dependent phase shift of the film-substrate interface occurring at the substrate band edge.

DOI: 10.1103/PhysRevB.65.085327 PACS number(s): 73.90.+f, 79.60.Dp

I. INTRODUCTION

Over the past decade, the quantum-well states (QWS's) associated with the electron confinement in thin metal films on various solid substrates have attracted considerable interests.[1–5] QWS's are important not only in studying low-dimensional physics but also for the present and future magnetic/electronic device applications through, for example, the oscillatory magnetic coupling and the giant magnetoresistance.[1,4,5] While a large number of studies have been devoted to QWS's in metal films on *metal* substrates, little is known about those on a *semiconductor* substrate.[1–21] This is due partly to the difficulty of growing epitaxial metal films, which are indispensable for any QWS study, on a semiconductor substrate. However, it has been found recently by scanning tunneling microscopy (STM) and low-energy electron-diffraction (LEED) studies that epitaxial metal films can be formed metastably on semiconductor substrates, for example, the Ag(111) films on the GaAs(110),[22,23] Si(111),[24,25] and Si(001) (Refs. 26–28) substrates. Such films are formed when Ag is deposited at a sufficiently low temperature below 130 K and a mild annealing up to 300–400 K is followed.[6,7,22–28] The existence of QWS's within such Ag films has been verified by photoemission spectroscopy.[6–9] We recently investigated the QWS's of the Ag(111) films on Si(001) in detail[6] and found that the binding energies E_B of these QWS's are described well by the standard model using the phase accumulation.[6]

In the present paper, we further investigate the in-plane dispersion $[E(\mathbf{k}_\parallel)]$ of the QWS's of the Ag(111) films on Si(111) and Si(001) with angle-resolved photoelectron spectroscopy (ARPES) using synchrotron radiation. Despite the success of the simple theoretical description of the QWS binding energies in the Ag(111)/Si(001) system,[6] the in-plane dispersion of the QWS's exhibits a significant deviation from the simple free-electron-like behavior expected.[29] The ARPES results show a significant enhancement of the in-plane effective mass ($m^*_\parallel$) with decreasing E_B of a QWS in both Ag/Si(111) and Ag/Si(001), and a splitting of a QWS into two subbands with different dispersions at off-normal emission in Ag/Si(001). The origins of such unexpected behaviors are discussed in terms of the substrate electronic structure affecting the phase shift at the film-substrate interface.

II. EXPERIMENTS

The experiments were performed on the vacuum ultraviolet beam line BL-7B (Research Center for Spectrochemistry, the University of Tokyo) at Photon Factory, Japan. The detailed experimental setup and the procedures for the sample preparation are the same as reported before.[6] The epitaxial Ag(111) films were prepared on the Si(001)2×1 and Si(111)7×7 substrates by evaporating Ag at 120 K and annealing subsequently up to ~300 K.[6,7,24–28] The LEED patterns exhibit only sharp Ag(111)1×1 spots for both Ag/Si(001) and Ag/Si(111) as shown in the insets of Figs. 1 and 4. This indicates the complete formation of well-ordered and smooth Ag films over the whole surface. The film thickness in the present study is given in terms of a Ag(111) monolayer ($1\ \mathrm{ML}=1.39\times10^{15}$ atoms/cm^2). All ARPES spectra of the Ag(111) films were taken at 120 K using linearly polarized synchrotron radiation at the photon energies ($h\nu$'s) of 22.7, 10.3, and 9.3 eV. The electron emission angles (θ_e's) and photon incident angles (θ_i's) are referred to the surface normal. Each spectrum shown below is normalized to the intensity above the Fermi level (E_F), which is proportional to the incident photon flux.

III. RESULTS AND DISCUSSION

Figure 1 shows a series of ARPES spectra for the 16-ML-thick Ag(111) film grown on Si(111)7×7. The spectra were taken at $h\nu=22.7$ eV along the $[10\bar{1}]$ axis of the Si substrate, which corresponds to $\bar{\Gamma}$-$\bar{M}$ line of the Ag(111)1×1 surface Brillouin zone (SBZ) (see the inset of Fig. 1). A Ag(111) surface state (denoted as SS) is observed just below E_F.[7,30] The dispersing QWS's are identified in a similar way

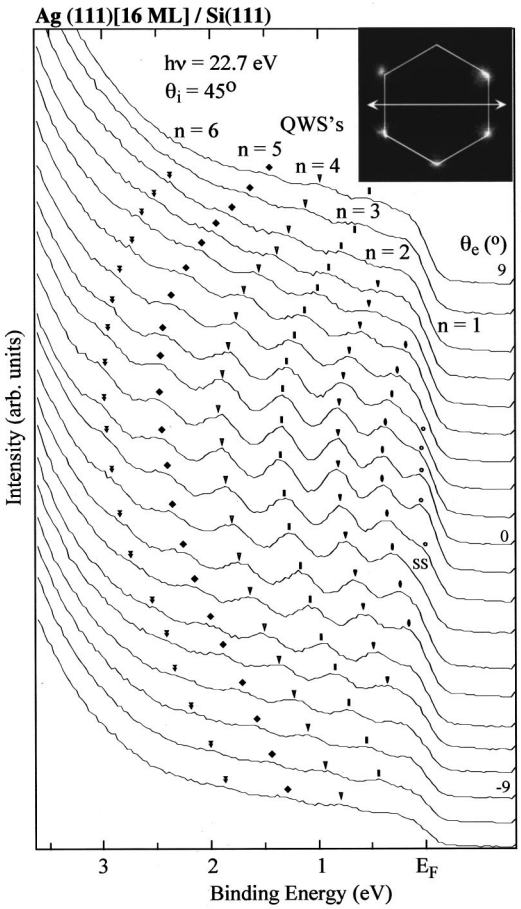

FIG. 1. ARPES spectra for a 16-ML-thick Ag(111) film on a Si(111) substrate taken along the $[10\bar{1}]$ axis of the substrate. The LEED pattern (at an electron energy of 125 eV) and the surface Brillouin zone of the Ag(111) surface are shown in the upper right part with the ARPES scan direction indicated (the arrow). The photon energy ($h\nu$) used is 22.7 eV and photon incident angle (θ_i) is 45°. The step in the emission angle (θ_e) is 1° between the neighboring spectra. The peak positions of a Ag(111) surface state (denoted as SS) and different quantum-well states assigned are marked with different symbols.

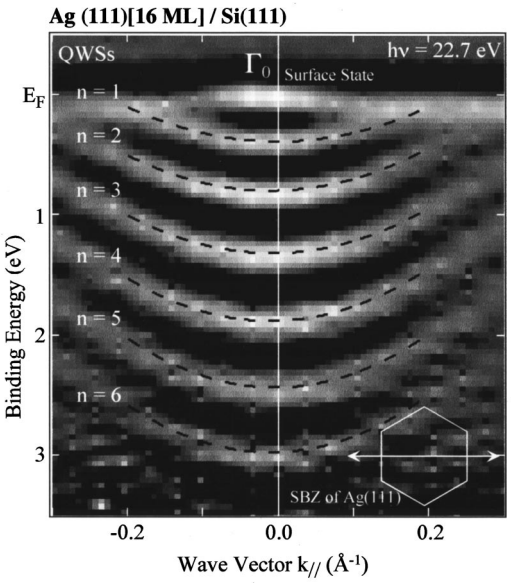

FIG. 2. The gray-scale E_B-$k_\parallel$ diagram for the 16-ML-thick Ag(111) film on a Si(111) substrate along the $[10\bar{1}]$ axis of the substrate taken from the ARPES scans at $h\nu = 22.7$ eV shown in Fig. 1. In this diagram the sign-inverted second derivative of the photoemission intensity is plotted, where the brightness roughly corresponds to the photoemission peak intensity above the background signal. The surface Brillouin zone (SBZ) of the Ag(111) surface and the ARPES scan direction (the arrow) are also indicated in the figure. The dashed lines are the parabolic fits of the QWS dispersions as explained in the text.

to the previous QWS studies on metal substrates.[20,21] The experimental dispersion curves for the spectral features observed in Fig. 1 are shown as the gray-scale E_B-$k_\parallel$ diagram in Fig. 2. In this diagram,[31] the spectral intensity is approximately represented by the brightness through taking the second derivative of each spectrum, which is then mapped into the $k_\parallel$ axis. In Fig. 2, one can clearly identify the parabolic dispersions of the QWS's. The dashed curves are the parabolic fits, $E(\mathbf{k}_\parallel) = h^2\mathbf{k}_\parallel{}^{*2}/(8\pi^2 m_\parallel{}^*) + E_0$, ($E_0$ is the binding energy at normal emission of $k_\parallel = 0$ and $m_\parallel{}^*$ is the in-plane effective mass), which are expected to be a good approximation for small $k_\parallel$ values.[20] Here, the fitting is performed for E_0 and $m_\parallel{}^*$ in the $k_\parallel$ range from -0.2 to 0.2 Å^{-1}. It is obvious that the simple parabolic fits match very well with the experimental data. In addition, it is also found that the size of in-plane dispersion decreases monotonically (i.e., $m_\parallel{}^*$ becomes larger) with a decrease of the QWS binding energy. That is, the dispersion curve of the $n=6$ QWS obviously has a larger curvature than that of $n=1$. For example, the fitted value of $m_\parallel{}^*$ is $0.51m_o$ (m_o; the free electron mass) for the $n=1$ QWS but decreases to $0.36m_o$ for $n=6$.

Figure 3 summarizes the $m_\parallel{}^*$ values as a function of E_0, which are obtained from the above parabolic fits to the ARPES data for the 16-ML-thick Ag film on Si(111). The results from the 14-ML-thick Ag films on Si(001) (see below) and on Cu(111) (see Ref. 20) are shown for comparison together with the bulk Ag data[20] (the solid line in Fig. 3). While $m_\parallel{}^*$ of the QWS's of Ag/Si(111) *increases* with decreasing E_0, that of Ag(111)/Cu(111) *decreases* monotonically in clear contrast.[20] That is, the relationship between $m_\parallel{}^*$ and E_0 clearly exhibits an opposite tendency for the Cu(111) and Si(111) substrates. The corresponding results for the QWS's of Ag/Si(001) is described in detail below.

The above results lead to a surprising conclusion that *the in-plane band structure of a thin Ag film depends on its substrate*. In order to confirm this statement further, we have performed similar ARPES measurements for the 14-ML-thick Ag(111) film grown on the Si(001)2×1 substrate. The study of the Ag(111) ultrathin film growth and the QWS's on Si(001) was reported in detail previously.[6] Figures 4–7 show the corresponding ARPES spectra and the gray-scale E_B-$k_\parallel$ diagrams taken at various photon energies of 22.7 (Figs. 4 and 5), 10.3 (Fig. 7), and 9.3 eV (Figs. 6 and 7). The ARPES scans are performed along the [110] axis of the Si(001) substrate. Since the Si(001) substrate has a double-domain 2×1 surface, the Ag(111) film grows in two different orien-

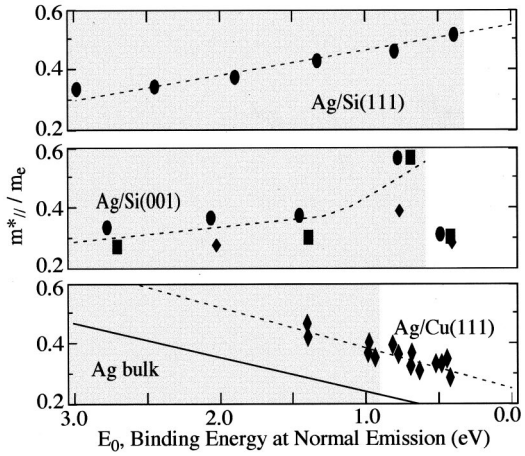

FIG. 3. In-plane effective mass, $m_{\|}$*, in ratios to the free-electron mass m_o as a function of the QWS binding energy at $k_{\|}=0$ for the Ag(111) film on the Si(111), Si(001) and Cu(111) [Ref. 20] substrates. The solid line at the bottom panel is the estimated values of the Ag(111) bulk. The dashed lines are the guides for tracing the experimental data. The shaded areas correspond to the substrate valence-band region. Solid circles, squares, and diamonds in the middle panel represent the data taken at $h\nu=22.7$, 10.3 and 9.3 eV, respectively.

tations rotated 90° from each other. Thus, the [110] axis corresponds to both $\overline{\Gamma}$-$\overline{K}$ and $\overline{\Gamma}$-$\overline{M}$ lines of the two different Ag(111)1×1 SBZ's (see the inset of Fig. 4). However, since the in-plane dispersion of the Ag *sp* band is isotropic within the limited $k_{\|}$ range probed, these two overlapping SBZ lines do not cause any significant ambiguity for the following data analyses. The apparent differences between the ARPES spectra taken with different photon energies (Figs. 4 and 6) are due to the matrix element effect (the energy- and *k*-dependent cross section) of the photoemission process.[6] As discussed before the drastic difference of the photoemission cross section is mainly due to the qualitatively different photoemission final states.[6] Similar to Figs. 1 and 2, the Ag(111) surface state is observed just below E_F in Figs. 4–7. As noted in Figs. 4–7, while the QWS of $n=1$ follows a normal parabolic dispersion, the $n=2$ QWS splits into two subbands at $k_{\|}\sim 0.1$ Å^{-1}; one band disperses to a lower binding energy in a roughly parabolic manner but the other to a slightly *higher* E_B. In Figs. 5 and 7, the dashed curves are the parabolic fits to the experimental dispersions. The parabolic fits match well with the experimental data for the QWS's of $n=1$, 3, 4, and 5. For the $n=2$ QWS, we performed the parabolic fit for the lower-energy subband only at 0.2 Å$^{-1}>k_{\|}>0.1$ Å^{-1} and -0.2 Å$^{-1}<k_{\|}<-0.1$ Å^{-1} since around $\overline{\Gamma}$ the energy positions of lower E_B subband are not clear and the higher E_B subband shows a completely different dispersion. This splitting will be discussed further below.

In order to summarize the different band dispersions of the QWS's of the Ag(111) films among the different substrates, let us now return to Fig. 3. In the case of Ag/Si(001), $m_{\|}$* monotonically increases as E_0 decreases down to ~0.6 eV, in qualitative consistency with the case of Ag/Si(111). However, the $m_{\|}$* value becomes significantly smaller when

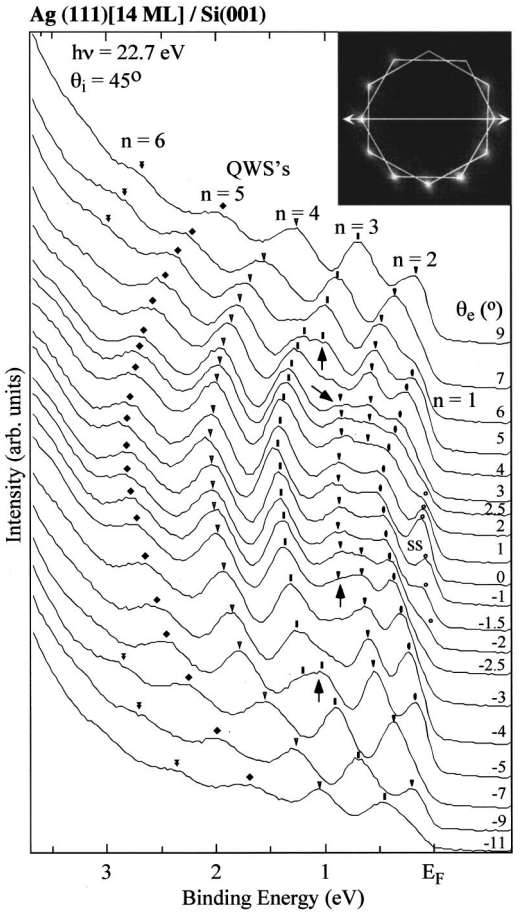

FIG. 4. Similar to Fig. 1 but for ARPES spectra of the 14-ML-thick double-domain Ag(111) film on a Si(001) substrate. The spectra were taken along the [110] axis of the Si(001) substrate at $h\nu=22.7$ eV and at the photon incident angle (θ_i) of 45° as indicated by the white arrow on the LEED pattern in the upper right part. The black arrows indicate the observed splitting of the quantum-well states (see text).

E_0 reaches ~0.5 eV for the $n=1$ QWS. In Fig. 3, there is a tendency that the $m_{\|}$* values obtained at $h\nu=22.7$ eV are slightly larger than those obtained from $h\nu=10.3$ and 9.3 eV for Ag/Si(001). This is a systematic experimental error due to the instrumental angular resolution, which becomes poorer at a higher photoelectron kinetic energy. In spite of such an error, the tendency of $m_{\|}$* is clearly shown to be invariant among three different photon energies. The $n=2$ QWS of Ag/Si(001) exhibits a largely different effective mass from those of other QWS's, which must be the influence of its splitting mentioned above. As evident in Fig. 3, the in-plane dispersion of QWS is obviously and significantly different among the different substrates, Cu(111), Si(111), and Si(001).

Although the Ag *sp* valence electrons are confined and quantized one dimensionally along the film normal in a thin Ag(111) film, the in-plane dispersion $E(\mathbf{k}_{\|})$ is expected to remain unaltered from those of a bulk Ag metal. For a bulk Ag(111) metal, $E(\mathbf{k}_{\|})$ is isotropic but the size of the dispersion becomes smaller with increasing E_B due to the finite hybridization with the $4d$ states at higher binding energy.[30]

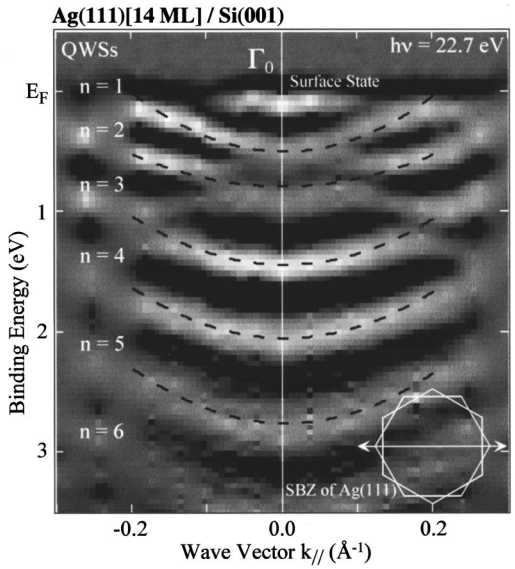

FIG. 5. Similar to Fig. 2 but for the 14-ML-thick double-domain Ag(111) film on the Si(001) substrate along taken from the ARPES spectra shown in Fig. 4.

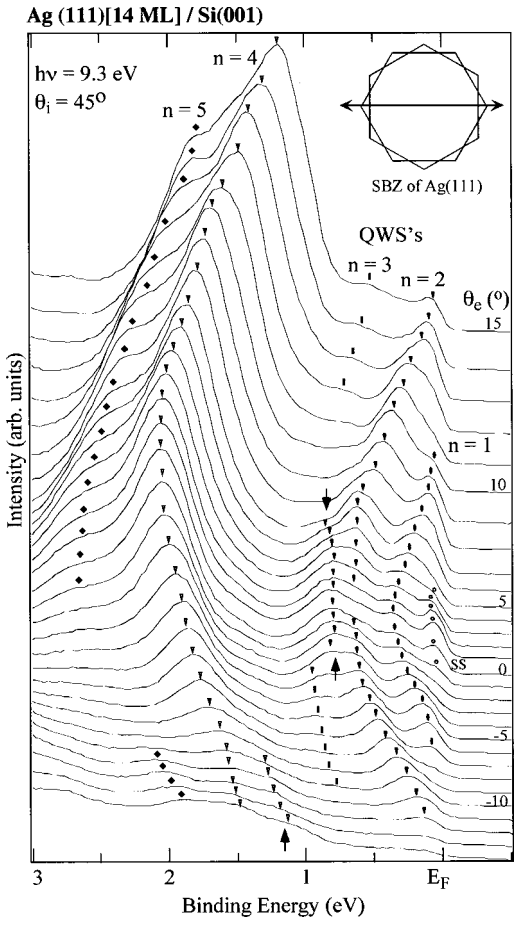

FIG. 6. Similar to Figs. 1 and 4 but for the 14-ML-thick double-domain Ag(111) film on Si(001) along the [110] axis at $h\nu = 9.3$ eV. The black arrows indicate the observed splitting of the quantum-well states (see text).

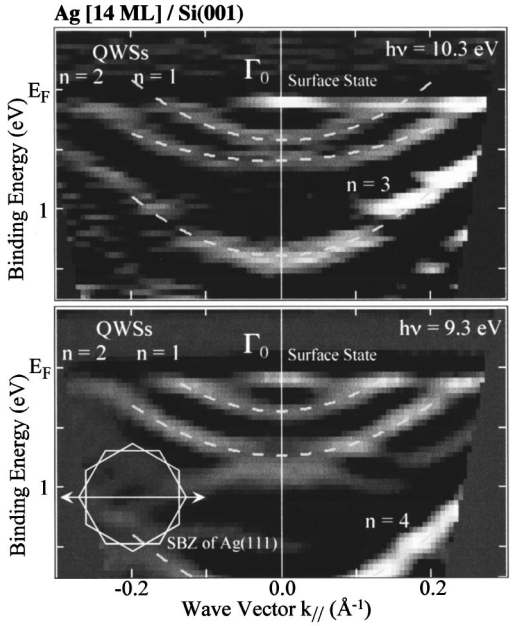

FIG. 7. Similar to Figs. 2 and 5 but for the 14-ML-thick double-domain Ag(111) film on Si(001) taken from the ARPES spectra shown in Fig. 6 (bottom panel) and from a similar set of spectra at $h\nu = 10.3$ eV, which is not shown here (top panel).

That is, $m_\parallel{}^*$ of the *sp* band increases with E_B as quantitatively estimated by Müller, Miller, and Chiang[20] (see the solid line in Fig. 3). Such an $m_\parallel{}^*$ tendency of the Ag bulk *sp* band was inferred to explain that of the QWS's in the Ag/Cu(111) system.[20] However, this is apparently not compatible to the present ARPES data of the Ag/Si(001) and Ag/Si(111) QWS's, which exhibit a completely opposite trend of $m_\parallel{}^*$ with respect to E_B.

A change of the in-plane dispersion might be possible due to the lateral strain of the grown film, which is naturally expected for a smooth film on a substrate with a finite lattice mismatch.[32] However, while the relaxation mechanism of the strain still remains to be studied, the lattice constants of Ag(111) films on Si(111) and Si(001) are reported to be very close to that of the bulk Ag metal with only few percent differences.[7,27,28] Within the tight-binding approximation, $m_\parallel{}^*$ is proportional to $a^{-2}\gamma(a)^{-1}$, where a is the nearest-neighbor distance and $\gamma(a)$ is the interatomic matrix elements.[33] Since for *s*- and *p*-like states $\gamma(a)$ have a a^{-2} dependence,[33] the strain effect on $m^*{}_\parallel$ of *sp* electrons could only be marginal. Moreover, the strain effect, if any, is naturally expected to be uniform over the whole energy region. This is obviously not the case with the present results on Ag/Si(001) and Ag/Si(111) QWS's with a qualitative different behavior from that of the Ag bulk and Ag/Cu(111).

Another factor to be considered in explaining the anomalous in-plane band dispersion may be the small in-plane coherent domain size of the film. However, such lateral size effect is unlikely since the present Ag(111) film has a domain size of larger than 200 Å as observed by STM and LEED,[6,7,24–28] which is far beyond the quantum limit of <50 Å.[34]

In a recent photoemission study of the Ag overlayers on

the $V(100)$ surface, Valla *et al.* observed a large deviation of the Ag *sp* in-plane band dispersion from the free-electron-like behavior.[15] They found that a QWS of 2-ML Ag film has $m_{\|}^*$ of as large as $3.1m_o$ at the vicinity of the $\bar{\Gamma}$ point and $m_{\|}^*$ further changes its sign when moving away from $\bar{\Gamma}$. From the similarity between such an unexpected dispersion of the QWS and that of the substrate $V(100)$ $3d$ band Valla *et al.* suggested a strong hybridization between these two electronic states. Such hybridization with the substrate electronic states may account for the unusual dispersions of the QWS's observed for Ag/Si(001) and Ag/Si(111).

In the case of the Si substrates, Si *sp* valence-band maximum (VBM) on $\bar{\Gamma}$ exists at $E_B \sim 0.3$ eV for Ag/Si(111) and at $E_B \sim 0.6$ eV for Ag/Si(001).[35–39] The shaded areas of Fig. 3 correspond to the substrate Si valence-band region below the VBM. When a QWS is located inside that energy range, it may interact or hybridize with the substrate electronic states. It seems that the unusual behaviors of $m_{\|}^*$ of Ag/Si(001) and Ag/Si(111) occur within such regions. We also note that the $m_{\|}^*$ values of Ag/Si(001) and Ag/Cu(111) becomes similar when the corresponding QWS's are located out of the substrate band region: the $n=1$ QWS of Ag/Si(001) has $m_{\|}^* = 0.3m_o$ at $E_B = 0.5$ eV (see Fig. 3). When the binding energy of the QWS increases to go into the Si bulk band region, $m_{\|}^*$ increases rapidly and then decreases gradually. Since the Si bulk bands have strong negative dispersions, the increase of QWS effective mass might be naturally expected from the hybridization with the Si bulk bands. Then the trend of effective-mass change (the part of ''gradual decrease'') suggests that the hybridization decreases upon increase of the binding energy from the valence-band maximum at least around the $\bar{\Gamma}$ point, where the effective mass was measured. This can also be expected, at least qualitatively, since the density of states of the Si bulk bands decreases from the valence-band maximum. However, the wave functions of the Ag(111) *sp* band and those of the Si(001) *sp* band are not expected to easily hybridize each other due to their difference of symmetry, that is, Λ_1 for Ag(111) and Δ_5, Δ'_2 for Si(001). Moreover it is not clear at all how the hybridization affects the in-plane band dispersion of a film as thick as 14–16 ML beyond the short screening length within a metal (a few monolayers at maximum).[40,41] A proper theoretical consideration is highly required for the band structures of the Ag films on the Si substrates in order to elucidate the origin of the unexpected substrate-dependent in-plane dispersions.

Another unusual aspect of the in-plane dispersion of the QWS's is the fact that the $n=2$ QWS of Ag/Si(001) shows a splitting into two subbands with largely different dispersions (see Figs. 4–7 and especially the arrows in Figs. 4 and 6). Although less obvious, similar splittings can be noticed for the $n=3$ and $n=4$ QWS as indicated by arrows in Figs. 4 and 6. In considering the origin of these split bands, we can exclude the possibility of observing the photoemission from the substrate surface. This is because (i) the recent STM and electron-diffraction studies[6,26–28] showed clearly that the Ag(111) film covers the whole terraces of the substrate surface uniformly and (ii) the electron mean free path for the corresponding photoelectrons reaches ~10 Å at most,[42] which amounts only to ~1/3 of the thickness of the present Ag(111) films. Thus, the unusual Ag QWS dispersion has to be attributed to the electronic states of the Ag film itself. One may suspect that the above splitting may be due to the mixed contributions from the parts of the Ag films with different thickness. This explanation is not plausible either since (i) the Ag films are shown to be uniform with only 1 or 2 ML height variation, (ii) the expected energy splitting from such height variation is much smaller than observed,[3,12] and (iii) the expected dispersion of the QWS's from a slightly different film thickness should still follow the parabolic dispersion in contrast to the present observation. Similar splittings are observed also for the Ag(111) films on Si(001) with different thickness.

We discuss the peculiar splitting of the QWS's observed for Ag/Si(001) in terms of the quantization condition of a QWS within the phase quantization rule:[1,3–6,10–12,14,15,18–20] $\phi_{\rm vac}(\mathbf{E}_n) + 2k(E_n)d + \phi_{\rm sub}(\mathbf{E}_n) = 2\pi(n-1)$ [n is the quantum number, k is the wave vector of the envelope function of a Bloch state perpendicular to the surface, d is the film thickness, and $\phi_{\rm vac}(\mathbf{E}_n)$ or $\phi_{\rm sub}(\mathbf{E}_n)$ is the phase shift at the film-vacuum or the film-substrate interface, respectively]. For a QWS at a certain thickness, the dispersion normal to the surface, $k(E_n)$, depends on the phase shifts. This is very similar to what is known for the dispersion of the so-called image-potential states of clean metal surfaces.[43] Thus, if $\phi_{\rm sub}(\mathbf{E}_n)$ or $\phi_{\rm vac}(\mathbf{E}_n)$ changes with $k_{\|}$, then the binding energy of a QWS would depend on $k_{\|}$ in addition to its own parabolic dispersion given by the bulk *sp* band structure. In particular, near the edge of the substrate bands $\phi_{\rm sub}(\mathbf{E}_n)$ can vary drastically between the outside and the inside of the substrate band, since the reflection at the band gap can be a rather perfect reflection as in the case of a hard wall potential but that at the bulk band cannot be perfect with the finite penetration of the incoming electrons into the substrate bulk band. This discontinuity of the phase shift is expected to distort the $E(\mathbf{k}_{\|})$ dispersion curve away from the free-electron-like behavior, bringing about a splitting or a discontinuity of the QWS dispersion at the bulk valence-band edge. Being consistent with this argument, it can be seen in Figs. 4–7 that the positions of the QWS energy splitting coincide reasonably well with the upper edge of the Si(001) valence bands.[35–37]

To speak more quantitatively, the splitting is observed at $k_{\|} \sim 0.1$ Å^{-1} and at $E_B \sim 0.8$ eV for the $n=2$ QWS (Figs. 4–7). Based on the one-dimensional potential-well model,[44] $\phi_{\rm sub}(\mathbf{E}_n)$ inside the Si valence band is treated as a constant, which is estimated experimentally to be $\phi_{\rm sub} \sim 0.7\pi$ for the $n=2$ QWS.[6] Within the band gap, $\phi_{\rm sub}(\mathbf{E}_n)$ is presumably π as in the case of a perfect Bragg reflection.[45] Then, the difference of the phase shift between the outside and the inside of the substrate band corresponds to 0.3π and the phase quantization rule gives $\Delta\phi_{\rm vac}(\mathbf{E}_n) + 2\ \Delta k(E_n)d = 0.3\pi$, where $\Delta\phi_{\rm vac}(\mathbf{E}_n)$ and $\Delta k(E_n)$ are the differences of $\phi_{\rm vac}(\mathbf{E}_n)$ and $k(E_n)$, respectively, between the outside and the inside of the substrate band at $E_B \sim 0.8$ eV. Since $\phi_{\rm vac}(\mathbf{E}_n)$ is not expected to depend on the Si band structure, the $\Delta\phi_{\rm vac}(\mathbf{E}_n)$ term should be negligible compared to the

$2\Delta k(E_n)d$ term. Although $\phi_{\rm vac}(\mathbf{E}_n)$ is energy dependent, in principle, which is, however, estimated to be negligibly small compared to the $\phi_{\rm sub}(\mathbf{E}_n)$ change within the WKB approximation.[46] $\Delta k(E_n)$ is then reduced to -0.015 Å^{-1} and the corresponding E_B discontinuity for the $n=2$ QWS is estimated to be -0.10 ± 0.04 eV from the k (E_n) relation obtained previously.[6] This value agrees reasonably well with the observed energy splitting of -0.13 ± 0.03 eV for the $n=2$ QWS (Figs. 4–7). Similar estimations were also made for the $n=3$ and 4 QWS's in agreement with the observed energy splittings; 0.13–0.18 and 0.21 eV for $n=3$ and 4, respectively. These estimations corroborate the idea of the phase-shift discontinuity at the substrate band edge in explaining the QWS splitting at off-normal emission. However, the simple model presented here is not complete enough to describe the detailed dispersion of the split QWS as observed for the higher energy branch of the $n=2$ QWS.

If we assume a similar relationship of the energy and the phase shift for Ag/Si(001) and Ag/Si(111), the E_B change of the QWS at the Si bulk band edge around $E_B\sim0.5$ eV [the $n=1$ QWS of Ag/Si(111)] is only -0.03 ± 0.03 eV. Such a small value is due to the flattening of the Ag *sp* band near the band top. Such small splitting and the broad QWS peak width may explain the reason that we do not observe any obvious QWS splitting for Ag/Si(111) as shown in Figs. 1 and 2.

IV. CONCLUSIONS

The in-plane dispersions of the QWS's have been extensively studied for the epitaxial Ag(111) films grown on Si(001) and Si(111) by angle-resolved photoemission. The QWS's show unexpected dispersions that deviate significantly from those expected from the bulk Ag *sp* band. That is, a QWS exhibits a splitting into two branches with largely different dispersions at off-normal emission and the in-plane effective mass, $m_\parallel$*, shows a significant enhancement with decreasing binding energy of a QWS. These behaviors are found to be closely related to the substrate band structure and the splitting is discussed in terms of the discontinuity of the reflection phase shift of the Ag/Si interface occurring at the valence-band edge of the substrate. Further investigations such as proper theoretical calculations are required for the better and quantitative understanding of the peculiar QWS properties observed presently.

ACKNOWLEDGMENTS

I.M. gratefully acknowledges the financial support from Photon Factory via Professor A. Yagishita and from the Japan Society for the Promotion of Science. H.W.Y. is supported by ASSRC funded by KOSEF, Brain Korea 21 program, and the Tera-level Nanodevices project (21 century Frontier Programs).

*Corresponding author. FAX: +82-2-312-7090. Email address: yeom@phya.yonsei.ac.kr

[1] T.-C. Chiang, Surf. Sci. Rep. **39**, 181 (2000).
[2] F. J. Himpsel, Science **283**, 1655 (1999).
[3] J. J. Paggel, T. Miller, and T.-C. Chiang, Science **283**, 1709 (1999).
[4] F. J. Himpsel, Surf. Rev. Lett. **2**, 81 (1995).
[5] J. E. Ortega, F. J. Himpsel, G. J. Mankey, and R. F. Willis, Surf. Rev. Lett. **4**, 361 (1997).
[6] I. Matsuda, H. W. Yeom, T. Tanikawa, K. Tono, T. Nagao, S. Hasegawa, and T. Ohta, Phys. Rev. B **63**, 125 325 (2001). The phase quantization equations [Eq. (1) and (2)] given in this reference were mistyped and the correct ones should be as follows: $\phi_{\rm vac}(\mathbf{E}_n)+2k(E_n)d+\phi_{\rm sub}(\mathbf{E}_n)=2\pi(n-1)$ (1) and $d_n(E_n)=[n-1+\phi_{\rm vac}(\mathbf{E}_n)/2\pi+\phi_{\rm sub}(\mathbf{E}_n)/2\pi]/[1-k_b(E_n)]$, with k_b (E_n) representing the bulk-band dispersion (2).
[7] G. Neuhold and K. Horn, Phys. Rev. Lett. **78**, 1327 (1997).
[8] D. A. Evans and K. Horn, Surf. Sci. **307–309**, 321 (1994).
[9] D. A. Evans, M. Alonso, R. Cimino, and K. Horn, Phys. Rev. Lett. **70**, 3483 (1993).
[10] M. Jalochowski, H. Knoppe, G. Lilienkamp, and E. Bauer, Phys. Rev. B **46**, 4693 (1992).
[11] A. L. Wachs, A. P. Shapiro, T. C. Hsieh, and T.-C. Chiang, Phys. Rev. B **33**, 1460 (1986).
[12] J. J. Paggel, T. Miller, and T.-C. Chiang, Phys. Rev. B **61**, 1804 (2000).
[13] D.-A. Luh, J. J. Paggel, T. Miller, and T.-C. Chiang, Phys. Rev. Lett. **84**, 3410 (2000).
[14] R. K. Kawakami, E. Rotenberg, E. J. Escorcia-Aparicio, H. J. Choi, T. R. Cummins, J. G. Tobin, N. V. Smith, and Z. Q. Qiu, Phys. Rev. Lett. **80**, 1754 (1998).
[15] T. Valla, P. Pervan, M. Milun, A. B. Hayden, and D. P. Woddruff, Phys. Rev. B **54**, 11 786 (1996).
[16] W. E. McMahon, T. Miller, and T.-C. Chiang, Phys. Rev. B **54**, 10 800 (1996).
[17] T. Miller, A. Samsavar, and T.-C. Chiang, Phys. Rev. B **50**, 17 686 (1994).
[18] N. V. Smith, Phys. Rev. B **49**, 332 (1994).
[19] J. E. Ortega, F. J. Himpsel, G. J. Mankey, and R. F. Willis, Phys. Rev. B **47**, 1540 (1993).
[20] M. A. Müller, T. Miller, and T.-C. Chiang, Phys. Rev. B **41**, 5214 (1990).
[21] S. Å. Lindgren and L. Wallden, Phys. Rev. Lett. **59**, 3003 (1987).
[22] A. R. Smith, K.-J. Chao, Q. Niu, and C.-K. Shih, Science **273**, 226 (1996).
[23] G. Neuhold, L. Bartels, J. J. Paggel, and K. Horn, Surf. Sci. **376**, 1 (1997).
[24] L. Huang, S. J. Chey, and J. H. Weaver, Surf. Sci. **416**, L1101 (1998).
[25] G. Meyer and K. H. Rieder, Appl. Phys. Lett. **64**, 3560 (1994); Surf. Sci. **331–333**, 600 (1995).
[26] S. Fölsch, G. Meyer, D. Winau, K. H. Rieder, M. H.-v. Hoegen, T. Schmidt, and M. Henzler, Phys. Rev. B **52**, 13 745 (1995).
[27] M. H.-v. Hoegen, T. Schmidt, M. Henzler, G. Meyer, D. Winau, and K. H. Rieder, Phys. Rev. B **52**, 10 764 (1995).
[28] M. H.-v. Hoegen, T. Schmidt, M. Henzler, G. Meyer, D. Winau, and K. H. Rieder, Surf. Sci. **331–333**, 575 (1995).
[29] H. Erschbaumer, A. J. Freeman, C. L. Fu, and R. Podloucky, Surf. Sci. **243**, 317 (1991).
[30] H. Wern, R. Courths, G. Leschik, and S. Hufner, Z. Phys. B:

Condens. Matter **60**, 293 (1985).
[31] H. W. Yeom, T. Abukawa, Y. Takakuwa, M. Nakamura, M. Kimura, A. Kakizaki, and S. Kono, Surf. Sci. Lett. **321**, L177 (1994); T. Abukawa, M. Sasaki, T. Hisamatsu, T. Goto, T. Kinoshita, A. Kakizaki, and S. Kono, Surf. Sci. **325**, 33 (1995).
[32] E. Bauer and J. van der Merwe, Phys. Rev. B **33**, 3657 (1986).
[33] W. A. Harrison, *Electronic Structure and the Properties of Solids* (Dover, New York, 1989).
[34] R. Fischer, Th. Fauster, and W. Steinmann, Phys. Rev. B **48**, 15 496 (1993).
[35] H. W. Yeom, I. Matsuda, K. Tono, and T. Ohta, Phys. Rev. B **57**, 3949 (1998).
[36] I. Matsuda, H. W. Yeom, K. Tono, and T. Ohta, Phys. Rev. B **59**, 15 784 (1999).
[37] I. Matsuda, H. W. Yeom, K. Tono, and T. Ohta, Surf. Sci. **438**, 231 (1999).
[38] S. Hasegawa, X. Tong, S. Takeda, N. Sato, and T. Nagao, Prog. Surf. Sci. **60**, 89 (1999).
[39] G. L. Ley, V. Yu. Aristov, L. Seehofer, T. Buslaps, R. L. Johnson, M. Gothelid, M. Hammar, U. O. Karlsson, S. A. Flodstroem, R. Feidenhans'l, M. Nielsen, E. Findeisein, and R. I. G. Uhrberg, Surf. Sci. **307–309**, 280 (1994).
[40] A. Zangwill, *Physics at Surface* (Cambridge University Press, Cambridge, 1988).
[41] H. Lüth, *Surface and Interfaces of Solid Materials* (Springer-Verlag, Berlin, 1995).
[42] S. Hüfner, *Photoelectron Spectroscopy*, 2nd ed. (Springer, New York, 1996).
[43] P. M. Echenique and J. B. Pendry, Prog. Surf. Sci. **32**, 111 (1990).
[44] P. Harrison, *Quantum Wells, Wires and Dots* (Wiley, New York, 2000).
[45] The present phase-shift estimation is qualitatively different from the well-known empirical formula [see N. V. Smith, N. B. Brookes, Y. Chang, and P. D. Johnson, Phys. Rev. B **49**, 332 (1994)]. This formula is, however, a purely empirical one, taken from the experimental results on metal-on-metal systems, which cannot explain the energy-dependent phase shift of the Ag/Si interface as shown before[6].
[46] E. G. McRae and M. L. Kane, Surf. Sci. **108**, 435 (1981).